

# Precision Measurements of the Nucleon Strange Form Factors at $Q^2 \sim 0.1 \text{ GeV}^2$

A. Acha,<sup>1</sup> K. A. Aniol,<sup>2</sup> D. S. Armstrong,<sup>3</sup> J. Arrington,<sup>4</sup> T. Averett,<sup>3</sup> S. L. Bailey,<sup>3</sup> J. Barber,<sup>5</sup> A. Beck,<sup>6</sup> H. Benaoum,<sup>7</sup> J. Benesch,<sup>8</sup> P. Y. Bertin,<sup>9</sup> P. Bosted,<sup>8</sup> F. Butaru,<sup>10</sup> E. Burtin,<sup>11</sup> G. D. Cates,<sup>12</sup> Y.-C. Chao,<sup>8</sup> J.-P. Chen,<sup>8</sup> E. Chudakov,<sup>8</sup> E. Cisbani,<sup>13</sup> B. Craver,<sup>12</sup> F. Cusanno,<sup>14</sup> R. De Leo,<sup>13</sup> P. Decowski,<sup>15</sup> A. Deur,<sup>8</sup> R. J. Feuerbach,<sup>8</sup> J. M. Finn,<sup>3</sup> S. Frullani,<sup>14</sup> S. A. Fuchs,<sup>3</sup> K. Fuoti,<sup>5</sup> R. Gilman,<sup>16,8</sup> L. E. Glesener,<sup>3</sup> K. Grimm,<sup>3</sup> J. M. Grames,<sup>8</sup> J. O. Hansen,<sup>8</sup> J. Hansknecht,<sup>8</sup> D. W. Higinbotham,<sup>8</sup> R. Holmes,<sup>7</sup> T. Holmstrom,<sup>3</sup> H. Ibrahim,<sup>17</sup> C. W. de Jager,<sup>8</sup> X. Jiang,<sup>16</sup> J. Katich,<sup>3</sup> L. J. Kaufman,<sup>5</sup> A. Kelleher,<sup>3</sup> P.M. King,<sup>18</sup> A. Kolarkar,<sup>19</sup> S. Kowalski,<sup>6</sup> E. Kuchina,<sup>16</sup> K. S. Kumar,<sup>5</sup> L. Lagamba,<sup>13</sup> P. LaViolette,<sup>5</sup> J. LeRose,<sup>8</sup> R. A. Lindgren,<sup>12</sup> D. Lhuillier,<sup>11</sup> N. Liyanage,<sup>12</sup> D. J. Margaziotis,<sup>2</sup> P. Markowitz,<sup>1</sup> D. G. Meekins,<sup>8</sup> Z.-E. Meziani,<sup>10</sup> R. Michaels,<sup>8</sup> B. Moffit,<sup>3</sup> S. Nanda,<sup>8</sup> V. Nelyubin,<sup>12,20</sup> K. Otis,<sup>5</sup> K. D. Paschke,<sup>5</sup> S. K. Phillips,<sup>3</sup> M. Poelker,<sup>8</sup> R. Pomatsalyuk,<sup>21</sup> M. Potokar,<sup>22</sup> Y. Prok,<sup>12</sup> A. Puckett,<sup>6</sup> Y. Qian,<sup>23</sup> Y. Qiang,<sup>6</sup> B. Reitz,<sup>8</sup> J. Roche,<sup>8</sup> A. Saha,<sup>8</sup> B. Sawatzky,<sup>10</sup> J. Singh,<sup>12</sup> K. Slifer,<sup>10</sup> S. Sirca,<sup>6</sup> R. Snyder,<sup>12</sup> P. Solvignon,<sup>10</sup> P. A. Souder,<sup>7</sup> M. Stutzman,<sup>8</sup> R. Subedi,<sup>24</sup> R. Suleiman,<sup>6</sup> V. Sulkosky,<sup>3</sup> W. A. Tobias,<sup>12</sup> P. E. Ulmer,<sup>17</sup> G. M. Urciuoli,<sup>14</sup> K. Wang,<sup>12</sup> R. Wilson,<sup>25</sup> B. Wojtsekhowski,<sup>8</sup> H. Yao,<sup>10</sup> Y. Ye,<sup>26</sup> X. Zhan,<sup>6</sup> X. Zheng,<sup>6</sup> S. Zhu,<sup>27</sup> and V. Ziskin<sup>6</sup>

(The HAPPEX Collaboration)

<sup>1</sup> Florida International University, Miami, Florida 33199, USA

<sup>2</sup> California State University, Los Angeles, Los Angeles, California 90032, USA

<sup>3</sup> College of William and Mary, Williamsburg, Virginia 23187, USA

<sup>4</sup> Argonne National Laboratory, Argonne, Illinois 60439, USA

<sup>5</sup> University of Massachusetts Amherst, Amherst, Massachusetts 01003, USA

<sup>6</sup> Massachusetts Institute of Technology, Cambridge, Massachusetts 02139, USA

<sup>7</sup> Syracuse University, Syracuse, New York 13244, USA

<sup>8</sup> Thomas Jefferson National Accelerator Facility, Newport News, Virginia 23606, USA

<sup>9</sup> Université Blaise Pascal/CNRS-IN2P3, F-63177 Aubièrre, France

<sup>10</sup> Temple University, Philadelphia, Pennsylvania 19122, USA

<sup>11</sup> CEA Saclay, DAPNIA/SPhN, F-91191 Gif-sur-Yvette, France

<sup>12</sup> University of Virginia, Charlottesville, Virginia 22904, USA

<sup>13</sup> INFN, Sezione di Bari and University of Bari, I-70126 Bari, Italy

<sup>14</sup> INFN, Sezione Sanità, 00161 Roma, Italy

<sup>15</sup> Smith College, Northampton, Massachusetts 01063, USA

<sup>16</sup> Rutgers, The State University of New Jersey, Piscataway, New Jersey 08855, USA

<sup>17</sup> Old Dominion University, Norfolk, Virginia 23529, USA

<sup>18</sup> University of Illinois, Urbana, Illinois 61801, USA

<sup>19</sup> University of Kentucky, Lexington, Kentucky 40506, USA

<sup>20</sup> St. Petersburg Nuclear Physics Institute of Russian Academy of Science, Gatchina, 188350, Russia

<sup>21</sup> Kharkov Institute of Physics and Technology, Kharkov 310108, Ukraine

<sup>22</sup> Jozef Stefan Institute, 1000 Ljubljana, Slovenia

<sup>23</sup> Duke University, Durham, North Carolina 27706, USA

<sup>24</sup> Kent State University, Kent, Ohio 44242, USA

<sup>25</sup> Harvard University, Cambridge, Massachusetts 02138, USA

<sup>26</sup> University of Science and Technology, Hefei, Anhui 230026, China

<sup>27</sup> China Institute of Atomic Energy, Beijing 102413, China

(Dated: August 18, 2006)

We report new measurements of the parity-violating asymmetry  $A_{PV}$  in elastic scattering of 3 GeV electrons off proton and  $^4\text{He}$  targets with  $\langle\theta_{lab}\rangle \sim 6.0^\circ$ . The  $^4\text{He}$  result ( $E_b = 2.75 \text{ GeV}$ ) is  $A_{PV} = (+6.40 \pm 0.23 \text{ (stat)} \pm 0.12 \text{ (syst)}) \times 10^{-6}$ . The proton result ( $E_b = 3.18 \text{ GeV}$ ) is  $A_{PV} = (-1.58 \pm 0.12 \text{ (stat)} \pm 0.04 \text{ (syst)}) \times 10^{-6}$ . These results significantly improve constraints on the electric and magnetic strange form factors  $G_E^s$  and  $G_M^s$ . We extract  $G_E^s = 0.002 \pm 0.014 \pm 0.007$  at  $\langle Q^2 \rangle = 0.077 \text{ GeV}^2$ , and  $G_E^s + 0.09 G_M^s = 0.007 \pm 0.011 \pm 0.006$  at  $\langle Q^2 \rangle = 0.109 \text{ GeV}^2$ , providing new limits on the role of strange quarks in the nucleon charge and magnetization distributions.

PACS numbers: 13.60.Fz, 11.30.Er, 13.40.Gp, 14.20.Dh

Over the past several decades, high energy lepton-nucleon scattering has revealed the rich structure of the nucleon over a wide range of length scales. In recent years, increasingly sensitive measurements of elas-

tic electron-nucleon scattering, mediated by photon exchange and  $Z^0$  exchange, has enabled the measurement of the electromagnetic and neutral weak form factors. These functions of the 4-momentum transfer  $Q^2$  charac-

terize nucleon charge and magnetization distributions.

In particular, the neutral weak form factor measurements provide a way to probe dynamics purely of the “sea” of virtual light (up, down and strange) quark-antiquark pairs that surrounds each valence quark in the nucleon. Since the  $Z^0$  boson couples to various quarks with different relative strengths compared to the photon, a combined analysis of proton and neutron electromagnetic form factor and proton neutral weak form factor measurements, along with the assumption of charge symmetry, allows the determination of the strange electric and magnetic form factors  $G_E^s$  and  $G_M^s$  [1].

The established experimental technique to measure the electron-nucleon weak neutral current amplitude is parity-violating electron scattering [2, 3]. Longitudinally polarized electron scattering off unpolarized targets can access a parity-violating asymmetry  $A_{PV} \equiv (\sigma_R - \sigma_L)/(\sigma_R + \sigma_L)$ , where  $\sigma_{R(L)}$  is the cross section for incident right(left)-handed electrons. Arising from the interference of the weak and electromagnetic amplitudes,  $A_{PV}$  increases with  $Q^2$  [4]. The accessible  $Q^2$  range to probe strange quark dynamics is 0.1 to 1 GeV<sup>2</sup>;  $A_{PV}$  ranges from 1 to 10s of parts per million (ppm).

Four experimental programs have published  $A_{PV}$  measurements that constrain linear combinations of  $G_E^s$  and  $G_M^s$  [5–11]. All data are mutually consistent. An intriguing pattern in the low  $Q^2$  behavior has marginal statistical significance. While non-zero values have not been definitively established at any value of  $Q^2$ , the accuracy of published results still leaves significant room for nucleon strangeness dynamics.

In this paper, we report two highly precise measurements of  $A_{PV}$  in elastic electron scattering off the proton and <sup>4</sup>He. For elastic electron-proton scattering, the chosen kinematic point is such that  $A_{PV}$  is sensitive to the linear combination  $G_E^s + 0.09G_M^s$ , while elastic electron-<sup>4</sup>He scattering is sensitive to only  $G_E^s$ . A simultaneous analysis of both measurements results in the most precise determination of  $G_E^s$  and  $G_M^s$  at  $Q^2 \sim 0.1$  GeV<sup>2</sup>.

The measurements were carried out in Hall A at the Thomas Jefferson National Accelerator Facility. A 35 to 55  $\mu$ A continuous-wave beam of longitudinally polarized  $\sim 3$  GeV electrons was incident on 20 cm long cryogenic targets. Elastically scattered electrons were focused into regions otherwise free of background by a pair of high resolution spectrometer systems. Detector segments made up of layers of quartz and brass intercepted the scattered flux. The resulting Cherenkov light was measured by photomultiplier tubes (PMTs). In each spectrometer arm, the <sup>4</sup>He elastic peak was focused into one single detector segment, while the <sup>1</sup>H elastic peak was divided over two separate detector segments, each with its own PMT. The experimental configuration is described in more detail in two previous publications [10, 11].

The polarized electron beam originated from a GaAs photocathode illuminated by circularly polarized light.

	Helium	Hydrogen
$A_Q$	-0.377 ppm	0.406 ppm
$A_{\text{Energy}}$	3 ppb	0.2 ppb
$\Delta x$	-0.2 nm	0.5 nm
$\Delta x'$	4.4 nrad	-0.2 nrad
$\Delta y$	-26 nm	1.7 nm
$\Delta y'$	-4.4 nrad	0.2 nrad

TABLE I: Cumulative beam asymmetries under polarization reversal in intensity and energy and beam differences in horizontal and vertical position and angle during the 2005 run.

The accelerated beam was directed into Hall A, where its intensity, energy and trajectory on target were inferred from the response of several monitoring devices. The sign of the laser circular polarization determined the electron helicity. This was selected pseudo-randomly at 15 Hz and then toggled to the opposing helicity after 33.3 ms, with each of these equal periods of constant helicity referred to as a “window”. The integrated response of each detector PMT and beam monitor was digitized and recorded for each window, and results for the two consecutive windows of opposing helicity were grouped together as a “pair” for asymmetry analysis. The average beam jitter at the 33 ms time scale was less than 700 ppm in intensity, 2 ppm in energy, 15  $\mu$ m in position and 6  $\mu$ rad in angle.

The beam monitors, target, detector components and the electronics were designed such that the fluctuations in the fractional difference in the PMT response between two consecutive windows was dominated by the scattered flux’s counting statistics for rates up to 100 MHz. This facilitated  $A_{PV}$  measurements with statistical uncertainty as small as 100 parts per billion (ppb) in a reasonable length of time. To keep spurious beam-induced asymmetries under control at this level, the configuration of the laser optics leading to the photocathode was carefully designed and monitored. Indeed, during the two month period of data collection with the Hydrogen target, the achieved level of control surpassed all previous benchmarks, as summarized in Table I.

The data collection took place over 55 days (<sup>4</sup>He) and 36 days (<sup>1</sup>H). A half-wave ( $\lambda/2$ ) plate was periodically inserted into the laser optical path which passively reversed the sign of the electron beam polarization. Roughly equal statistics were thus accumulated with opposite signs for the measured asymmetry, which suppressed many systematic effects. There were 121 (<sup>4</sup>He) and 41 (<sup>1</sup>H) such reversals. The dataset between two successive  $\lambda/2$  reversals is referred to as a “slug”.

First, loose requirements were imposed on beam quality, removing periods of beam intensity, position, or energy instability. This left about 95% of the data sample for further analysis. No helicity-dependent cuts were applied. The final data sample consisted of  $35.0 \times 10^6$  (<sup>4</sup>He) and  $26.4 \times 10^6$  (<sup>1</sup>H) pairs.

The right-left helicity asymmetry in the integrated de-

tector response, normalized to the beam intensity, was computed for each window pair to form the raw asymmetry  $A_{\text{raw}}$ . The dependence of  $A_{\text{raw}}$  on fluctuations in the five correlated beam parameter differences  $\Delta x_i$  is quantified as  $A_{\text{beam}} = \sum c_i \Delta x_i$ . The electroweak physics of the signal and backgrounds is contained in  $A_{\text{corr}} = A_{\text{raw}} - A_{\text{beam}}$ . These distributions were studied to evaluate statistical and systematic errors.

The  $A_{\text{corr}}$  window-pair distributions for the two complete data samples had negligible non-Gaussian tails over more than 4 orders of magnitude with an RMS of 1130 ppm ( $^4\text{He}$ ) and 540 ppm ( $^1\text{H}$ ); the dominant source of noise in the PMT response was counting statistics. To further test that the data behaved statistically and the errors were being accurately calculated,  $A_{\text{corr}}$  averages and statistical errors for typical one hour runs, consisting of about 50k window-pairs each, were studied. These two sets of roughly 400 average  $A_{\text{corr}}$  values, normalized by the corresponding statistical error, each populated a Gaussian distribution of unit variance as expected.

Systematic effects in  $A_{\text{beam}}$  estimations were studied. When averaged over all detector segments, the coefficients  $c_i$  that quantify the  $A_{\text{raw}}$  beam parameter sensitivity were much smaller than those for individual detector segments due to the symmetric geometry of the apparatus. Limits on systematic variations in  $c_i$  in the range of 10 to 30% were set by inspecting residual correlations of  $A_{\text{corr}}$ 's of individual detector segments with helicity-correlated beam asymmetries.

Another important validation was to use two independent methods to calculate  $c_i$ . The first relied on linear regression of the observed response of the detector PMTs to intrinsic beam fluctuations. The other used a calibration subset of the data where the beam was modulated over its entire parameter space using steering magnets and an accelerating cavity by amounts large compared to intrinsic beam fluctuations. Differences in the two  $A_{\text{beam}}$  calculations were always much smaller than corresponding statistical errors.

Final  $A_{\text{corr}}$  results were calculated using the beam modulation technique and are summarized in Table II. Due to the excellent control of beam parameter differences  $\Delta x_i$  summarized in Table I,  $A_{\text{corr}} - A_{\text{raw}}$  values are of the order of, and typically much smaller than, the corresponding statistical errors. Under  $\lambda/2$  reversal, the absolute values of  $A_{\text{corr}}$  are consistent within statistical errors. The reduced  $\chi^2$  for  $A_{\text{corr}}$  “slug” averages is close to one in every case, indicating that any residual beam-related systematic effects were small and randomized over the time period of  $\lambda/2$  reversals (typically 5 to 10 hours). The final  $A_{\text{corr}}$  results respectively are  $A_{\text{corr}}^{\text{He}} = +5.25 \pm 0.19(\text{stat}) \pm 0.05(\text{syst})$  ppm and  $A_{\text{corr}}^{\text{H}} = -1.42 \pm 0.11(\text{stat}) \pm 0.02(\text{syst})$  ppm.

The physics asymmetry  $A_{\text{phys}}$  is formed from  $A_{\text{corr}}$  by correcting for the beam polarization  $P_b$ , background fractions  $f_i$  with asymmetries  $A_i$  and finite kinematic accep-

	IHWP OUT		IHWP IN		BOTH	
$^4\text{He}$	(DOF = 59)		(DOF = 60)		(DOF = 120)	
	Asym	$r\chi^2$	Asym	$r\chi^2$	Asym	$r\chi^2$
$A_{\text{raw}}$	$4.80 \pm 0.27$	0.75	$-5.41 \pm 0.27$	1.12	$5.10 \pm 0.19$	0.95
$A_{\text{corr}}$	$5.12 \pm 0.27$	0.78	$-5.38 \pm 0.27$	1.07	$5.25 \pm 0.19$	0.92
$^1\text{H}$	(DOF = 20)		(DOF = 19)		(DOF = 40)	
	Asym	$r\chi^2$	Asym	$r\chi^2$	Asym	$r\chi^2$
$A_{\text{raw}}$	$-1.40 \pm 0.15$	0.73	$1.42 \pm 0.15$	1.04	$-1.41 \pm 0.11$	0.86
$A_{\text{corr}}$	$-1.41 \pm 0.15$	0.81	$1.43 \pm 0.15$	1.02	$-1.42 \pm 0.11$	0.89

TABLE II: Raw and corrected detector asymmetries (in ppm) and reduced “slug” chi-squares ( $r\chi^2$ ), broken up by Insertable Half-Wave Plate (IHWP) reversals

Correction (ppb)	Helium	Hydrogen
Beam Asyms.	$183 \pm 59$	$-10 \pm 17$
Target windows	$113 \pm 32$	$7 \pm 19$
Helium QE	$12 \pm 20$	-
Rescatter	$20 \pm 15$	$2 \pm 4$
Nonlinearity	$0 \pm 58$	$0 \pm 15$
Scale Factor	Helium	Hydrogen
Acceptance $K$	$1.000 \pm 0.001$	$0.979 \pm 0.002$
$Q^2$ Scale	$1.000 \pm 0.009$	$1.000 \pm 0.017$
Polarization $P_b$	$0.844 \pm 0.008$	$0.871 \pm 0.009$

TABLE III: Corrections to  $A_{\text{corr}}$  and systematic errors

tance  $K$  as follows:

$$A_{\text{phys}} = \frac{K}{P_b} \frac{A_{\text{corr}} - P_b \sum_i A_i f_i}{1 - \sum_i f_i}. \quad (1)$$

These corrections are summarized in Table III. The first line lists the cumulative  $A_{\text{beam}}$  corrections discussed above, scaled by  $K/P_b$ . We now elaborate on the rest of the corrections.

A powerful feature of the apparatus is the spectrometers’ ability to focus the elastically scattered electrons into a compact region. Indeed, much less than 1% of the flux intercepted by the detectors originated from inelastic scattering in the target cryogen. Figure 1 shows charged particle spectra obtained with dedicated low-intensity runs and measured by drift chambers in front of the detectors. The dominant background was quasi-elastic scattering from target windows, separately measured using an equivalent aluminum target and computed to be  $1.8 \pm 0.2\%$  ( $^4\text{He}$ ) and  $0.76 \pm 0.25\%$  ( $^1\text{H}$ ).

An electron must give up more than 19 MeV to break up the  $^4\text{He}$  nucleus and undergo quasi-elastic scattering off nucleons. Figure 1 shows that the quasi-elastic threshold lies beyond the edge of the detector. A limit of  $0.15 \pm 0.15\%$  on this background was placed by detailed studies of the low-intensity data. For  $^1\text{H}$ , the  $\pi^0$  threshold is beyond the extent of the plot; direct background from inelastic scattering is thus negligible.

Background from rescattering in the spectrometer apertures was studied by varying the spectrometer momentum in dedicated runs to measure inelastic spectra

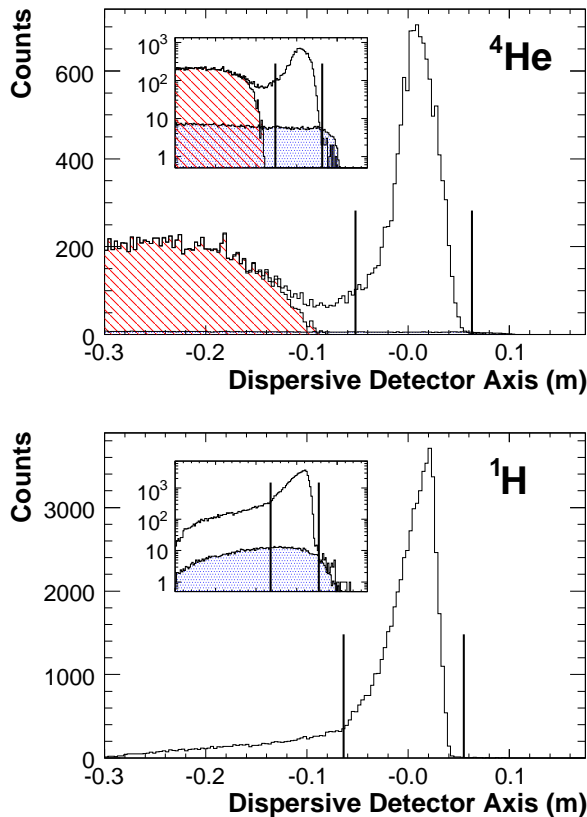


FIG. 1: Single-particle spectra obtained in dedicated low-current runs. The insets show the same spectra on a logarithmic scale. The vertical lines delineate the range of the detectors. Inelastic scattering from  ${}^4\text{He}$  is entirely contained in the hatched area. The shaded regions, visible only in the log plots, show the contribution from target windows.

and to obtain the detector response as a function of scattered electron energy under running conditions. From these two distributions, the rescattering background was estimated to be  $0.25 \pm 0.15\%$  ( ${}^4\text{He}$ ) and  $0.10 \pm 0.05\%$  ( ${}^1\text{H}$ ).

For each source of background, a theoretical estimate for  $A_{PV}$  was used, with relative uncertainties taken to be 100% or more to account for kinematic variations and resonance contributions. The resulting corrections and the associated errors are shown in Table III. Upper limits on rescattering contributions from exposed iron in the spectrometer led to an uncertainty of 5 ppb.

Nonlinearity in the PMT response was limited to 1% in bench-tests that mimicked running conditions. The relative nonlinearity between the PMT response and those of the beam intensity monitors was limited to 2% by data studies. The acceptance correction  $K$  accounted for the non-linear dependence of the asymmetry with  $Q^2$ . A significant systematic error in  $\langle Q^2 \rangle$  is from the determination of the absolute scale of  $\theta_{lab}$ . A nuclear recoil technique with a dedicated calibration run using a water cell target [10] was used to set a scale error on  $\langle Q^2 \rangle$  of  $< 0.2\%$ .

The beam polarization was continuously monitored by a Compton polarimeter. Helicity-dependent asymmetries in the recoil Compton electrons yielded  $P_b^{\text{He}} = (0.844 \pm 0.008)$  and  $P_b^{\text{H}} = (0.871 \pm 0.009)$ , averaged over the duration of the respective runs. The results were consistent, within systematic uncertainties, with those obtained from recoil Compton photon asymmetries, and with dedicated measurements using Møller scattering in the experimental hall and Mott scattering at low energy. The error in  $A_{\text{corr}}$  due to a vertical component of the beam polarization and imperfect cancellation of a transverse asymmetry was limited to a negligible level through dedicated studies using a fully vertical beam polarization.

After all corrections, the new  $A_{\text{phys}}$  results are:

$$A_{\text{phys}}^{\text{He}} = +6.40 \pm 0.23 \text{ (stat)} \pm 0.12 \text{ (syst)} \text{ ppm.}$$

$$A_{\text{phys}}^{\text{H}} = -1.58 \pm 0.12 \text{ (stat)} \pm 0.04 \text{ (syst)} \text{ ppm.}$$

The theoretical predictions  $A_{\text{NS}}^{\text{He}}$  and  $A_{\text{NS}}^{\text{H}}$  with  $G^s = 0$  were estimated using the formalism in [3] and described in our previous publications [10, 11]. All electroweak radiative corrections were calculated using the  $(\overline{\text{MS}})$  renormalization scheme. Purely electromagnetic radiative corrections were negligible due to the small fractional momentum acceptance of the spectrometers and the spin independence of soft photon emission [12].

Assuming a pure isoscalar  $0^+ \rightarrow 0^+$  transition,  $A_{\text{NS}}^{\text{He}}$  is completely independent of nuclear structure and determined purely by electroweak parameters. D-state and isospin admixtures and meson exchange currents are negligible at the level of the experimental fractional accuracy of  $\sim 3\%$  [13]. For our kinematics ( $E_b=2.75$  GeV,  $\langle Q^2 \rangle \sim 0.077$  GeV $^2$ ) we obtain  $A_{\text{NS}}^{\text{He}} = +6.37$  ppm.

A phenomenological fit to the world data of the electromagnetic form factors at low  $Q^2$  [14] was used to calculate  $A_{\text{NS}}^{\text{H}}$ , with uncertainties governed by data near  $Q^2 \sim 0.1$  GeV $^2$ . The only significant difference from values used in our previous publication [11] is for  $G_E^{\gamma n} = 0.037$ , with a 10% relative uncertainty based on new data from the BLAST experiment [15]. For our kinematics ( $E_b=3.18$  GeV and  $\langle Q^2 \rangle \sim 0.109$  GeV $^2$ ) we obtain  $A_{\text{NS}}^{\text{H}} = -1.66 \pm 0.05$  ppm. This includes a contribution from the axial hadronic current, and associated radiative corrections [16], of  $-0.037 \pm 0.018$  ppm.

Comparing our results to the theoretical expectations, we extract  $G_E^s = 0.002 \pm 0.014 \pm 0.007$  at  $Q^2 = 0.077$  GeV $^2$  and  $G_E^s + 0.09G_M^s = 0.007 \pm 0.011 \pm 0.004 \pm 0.005$  (FF) at  $Q^2 = 0.109$  GeV $^2$ , where the uncertainties in the nucleon electromagnetic form-factors govern the last error. Figure 2 displays the combined result for these and previously reported measurements using the same apparatus [10, 11], evolved to a common  $Q^2 = 0.1$  GeV $^2$  while assuming that  $G_E^s \propto Q^2$  and that  $G_M^s$  is constant. The values  $G_E^s = -0.005 \pm 0.019$  and  $G_M^s = 0.18 \pm 0.27$ , with a correlation coefficient of  $-0.87$ , are obtained. The

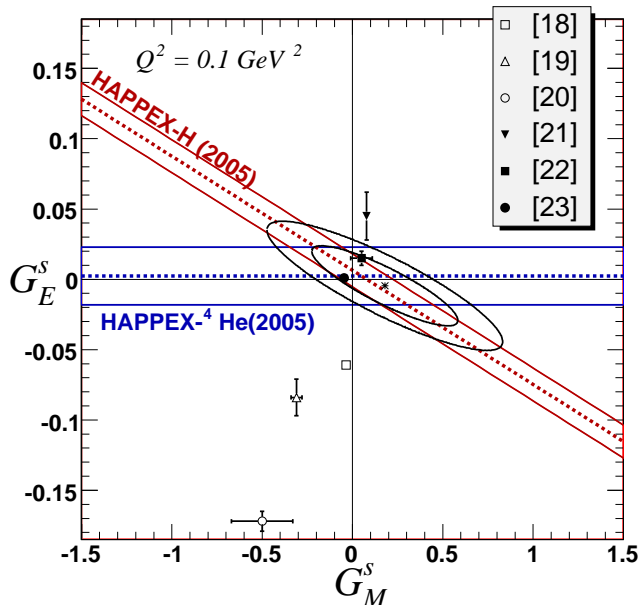


FIG. 2: 68 and 95% C.L. constraints in the  $G_E^s - G_M^s$  plane from both 2004 [10, 11] and 2005 (this Letter) data from this apparatus, along with various theoretical predictions. The 1- $\sigma$  bands (a quadrature sum of statistical and systematic errors) from the new results are also shown.

results are quite insensitive to axial form factor variations, as evidenced by the negligible change induced by an alternate fit similar to that in [17], where the axial form factor constraints are obtained from other  $A_{PV}$  data.

Figure 2 also displays predictions from various theoretical models [18–23]. Those that predict little strange quark dynamics in the vector form factors are favored [22, 23]. Other measurements [5, 8, 9] that had suggested larger strangeness effects are consistent with the fit in Fig. 2 within quoted uncertainties. Due to the improved statistical precision and lower axial form factor sensitivity of our fit result, adding these published measurements does not alter our conclusions.

In summary, we have reported the most precise constraints on the strange form factors at  $Q^2 \sim 0.1 \text{ GeV}^2$ . The results, consistent within errors with other  $A_{PV}$  measurements, leave little room for nucleon strangeness dynamics at low  $Q^2$ . It now becomes a challenge for various theoretical approaches to reconcile these results and en-

hance our understanding of nucleon structure.

We wish to thank the entire staff of JLab for their efforts to develop and maintain the polarized beam and the experimental apparatus. This work was supported by DOE contract DE-AC05-84ER40150 Modification No. M175, under which the Southeastern Universities Research Association (SURA) operates JLab, and by the Department of Energy, the National Science Foundation, the INFN (Italy), and the Commissariat à l'Énergie Atomique (France).

- 
- [1] D.B. Kaplan and A. Manohar, Nucl. Phys. B **310**, 527 (1988).
  - [2] R.D. McKeown, Phys. Lett. B **219**, 140 (1989).
  - [3] M.J. Musolf *et al.*, Phys. Rep. **239**, 1 (1994).
  - [4] Ya.B. Zel'dovich, Sov. Phys. JETP, **36**, 964 (1959).
  - [5] D.T. Spayde *et al.*, Phys. Lett. B **583**, 79 (2004).
  - [6] K.A. Aniol *et al.*, Phys. Lett. B **509**, 211 (2001); K. A. Aniol *et al.*, Phys. Rev. C **69**, 065501 (2004).
  - [7] F.E. Maas *et al.*, Phys. Rev. Lett. **93**, 022002 (2004).
  - [8] F.E. Maas *et al.*, Phys. Rev. Lett. **94**, 152001 (2005).
  - [9] D.S. Armstrong *et al.*, Phys. Rev. Lett. **95**, 092001 (2005).
  - [10] K.A. Aniol *et al.*, Phys. Rev. Lett. **96**, 022003 (2006).
  - [11] K.A. Aniol *et al.*, Phys. Lett. B **635**, 275 (2006).
  - [12] L.C. Maximon and W. C. Parke, Phys. Rev. C **61**, 045502 (2000).
  - [13] M.J. Musolf, R. Schiavilla and T.W. Donnelly, Phys. Rev. C **50**, 2173 (1994); S. Ramavataram, E. Hadjimichael and T.W. Donnelly, Phys. Rev. C **50**, 1175 (1994); M.J. Musolf and T.W. Donnelly, Phys. Lett. B **318**, 263 (1993).
  - [14] J. Friedrich and Th. Walcher, Eur. Phys. J. A **17**, 607 (2003).
  - [15] V. Ziskin, PhD. thesis, Massachusetts Institute of Technology, 2005.
  - [16] S.-L. Zhu *et al.*, Phys. Rev. D **62**, 033008 (2000).
  - [17] R. Young *et al.*, nucl-ex/0604010.
  - [18] N.W. Park and H. Weigel, Nucl. Phys. A **451**, 453 (1992).
  - [19] H.W. Hammer, U.G. Meissner, and D. Drechsel, Phys. Lett. B **367**, 323 (1996).
  - [20] H.W. Hammer and M.J. Ramsey-Musolf, Phys. Rev. C **60**, 045204 (1999).
  - [21] A. Silva *et al.*, Phys. Rev. D **65**, 014015 (2001).
  - [22] R. Lewis *et al.*, Phys. Rev. D **67**, 013003 (2003).
  - [23] D.B. Leinweber *et al.*, Phys. Rev. Lett. **94**, 212001 (2005); D.B. Leinweber *et al.*, Phys. Rev. Lett. **97**, 022001 (2006).